Scientia Iranica B (2013) 20(5), 1528–1537

SCIENTIA IRANICA

Sharif University of Technology
Scientia Iranica
Transactions B: Mechanical Engineering
www.scientiairanica.com

Numerical energy separation analysis on the commercial Ranque-Hilsch vortex tube on basis of application of different gases

N. Pourmahmoud[a,*], S.E. Rafiee[b], M. Rahimi[b] and A. Hassanzadeh[a]

a. *Department of Mechanical Engineering, Urmia University, Urmia, Iran.*
b. *Department of Mechanical Engineering, Urmia University of Technology, Urmia, Iran.*

Received 25 May 2012; accepted 27 May 2013

KEYWORDS
Ranque-Hilsch Vortex tube;
Numerical study;
Energy separation;
Inlet gases.

Abstract. In this numerical study, energy separation analysis of a Ranque-Hilsch Vortex Tube (RHVT) has been investigated for different conditions such as operation of machine under applying different inlet gases. The utilized gases in this study are nitrogen dioxide (NO_2), carbon dioxide (CO_2), oxygen (O_2), nitrogen (N_2) and air. The cooling and heating performance in a commercial vortex tube for the mentioned gases has been described in details and illustrated by different curves. The present three-dimensional (3D) Computational Fluid Dynamic (CFD) model is a steady axisymmetric model that employs standard k-ε turbulence model to perform the computational procedure of results. Various key parameters including cold and hot exit temperature differences and energy separation rates are described numerically. The results show that NO_2 enhances the greatest amount of cooling and heating capacity among investigated gases. Some of the numerical results are validated by available experimental data. Furthermore, a comprehensive comparison is performed in this article between two different kinds of boundary conditions for cold and hot exhausts, i.e. pressure-outlet and pressure-far-field.

1. Introduction

The vortex tube is a simple device without any moving parts that separates a pressurized gas into hot and cold streams. A schematic drawing of a typical vortex tube and its performance is shown in Figure 1. A vortex tube includes different parts like one or more inlet nozzles, a vortex chamber, a cold end orifice, a control valve at hot end and a working tube. When pressured gas is injected into the vortex chamber tangentially via the inlet nozzles, a powerful rotational flow field is established.

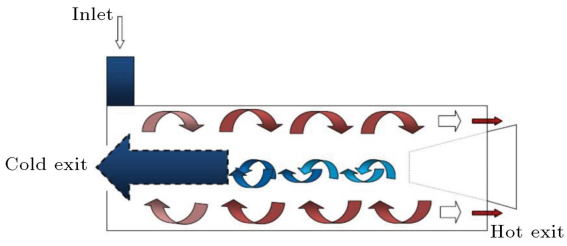

Figure 1. A schematic drawing of Ranque-Hilsch vortex tube.

The gas is expanded and cooled when it swirls to the center of the vortex chamber. After occurrence of the energy separation in the vortex tube, the pressured inlet air stream was separated into two different air streams (cold and hot streams). The "cold exit or cold

*. *Corresponding author. Tel.: +98 914 345 6358, Fax: +98 441 345 2032*
E-mail addresses: n.pormahmod@urmia.ac.ir (N. Pourmahmoud)); s.e.rafiee@mee.uut.ac.ir (S.E. Rafiee); m.rahimi@mee.uut.ac.ir (M. Rahimi); st_a.hassanzadeh@urmia.ac.ir (A. Hassanzadeh)

orifice" is located near the inlet nozzle, and at the other side of the working tube, there is a changeable flow restriction, namely the conical control valve. The hot outer shell of the compressed gas escapes through the conical valve at the end of the tube, and the remaining gas returns in an inner vortex and leaves through the cold exit orifice. Opening the hot valve reduces the cold airflow and closing the hot valve increases the cold airflow. Cold mass fraction or α can be defined as:

$$\alpha = \frac{\dot{m}_c}{\dot{m}_i}. \tag{1}$$

In this equation, $\dot{m}_c$ is the mass flow rate at the cold exit and $\dot{m}_i$ is the inlet flow rate.

Vortex tube was first created by Ranque in 1932 [1] when he was studying processes in a dust separation cyclone. The German physicist Rudolf Hilsch [2] improved the design of this apparatus. The detailed procedure of energy separation phenomenon is not completely understood yet. In the present investigation, instantaneous procedure of energy separation is illustrated in a vortex tube by computational data. The vortex tube has been the subject of many studies. Some of these investigations are briefly mentioned in this article. Kurosaka [3] stated that the temperature separation is a result of acoustic streaming effect. Stephan et al. [4] maintained that Gortler vortices form on the inside wall of the working tube and drive the fluid motion. Dincer et al. [5] experimentally investigated the distinction between hot and cold streams of vortex tubes with different length to diameter ratios (L/D). Ahlborn and Gordon [6] explained an embedded secondary circulation. Akhesmeh et al. [7] made a 3D CFD model in order to study the variation of velocity, pressure and temperature inside a vortex tube. Their results obtained upon numerical approach emphasized comprehensively on the mechanism of hot peripheral flow and a reversing cold inner core flow formation. Aljuwayhel et al. [8] utilized a fluid dynamics model of a vortex tube to realize the procedure that operates the temperature separation phenomena. Skye et al. [9] employed a model similar to that of Aljuwayhel et al. [8]. Bramo and Pourmahmoud [10] investigated, numerically, the effect of length to diameter ratio (L/D) and stagnation point occurrence importance in flow patterns. Chang [11] performed an experimental investigation of vortex tube refrigerator with a divergent hot tube. Polat and Kirmaci [12] performed an investigation about determining gas type in counter flow vortex tube using pairwise fisher score attribute reduction method. Pourmahmoud et al. [13,14] investigated numerically the effect of helical nozzles on the performance of vortex tube and their priority on the straight ones. Khazaei et al. [15] investigated, numerically, the effect of gas properties and geometrical parameters on performance of vortex tube by a 2D CFD model. They also showed that the hot outlet size and its shape do not affect the energy distribution in the vortex tube, and a very small diameter will decrease the temperature separation.

In the present work, assuming the advantages of using different inlet gases on the energy separation and their considerable role on the creation of maximum cooling capacity of machine, the kind of operating gases was concentrated. This research believes that choosing an appropriate gas type is one of the important thermo physical parameters. So far, numerical investigations towards inlet gases has not been done, but the importance of this object can be regarded as an interesting theme of research, so that the machine would operate in a way that maximum cooling effect or maximum refrigeration capacity is provided.

2. Governing equations

The compressible turbulent and highly rotating flow inside the vortex tube is assumed to be three-dimensional and steady state, and employs the standard k-ε turbulence model based on finite volume method. The RNG k-ε turbulence model and more advanced turbulence models such as the Reynolds stress equations were also investigated, but these models could not be converged for this simulation [8]. Bramo and Pourmahmoud [10] showed that because of the good agreement between the numerical results and the experimental data, the k-ε model can be selected to simulate the effect of turbulence inside the computational domain. Consequently, the governing equations are arranged by the conservation of mass, momentum and energy equations, which are given by:

$$\frac{\partial}{\partial x_j}(\rho u_j) = 0, \tag{2}$$

$$\frac{\partial}{\partial x_j}(\rho u_i u_j) = -\frac{\partial p}{\partial x_i} + \frac{\partial}{\partial x_j}\left[\mu\left(\frac{\partial u_i}{\partial x_j} + \frac{\partial u_j}{\partial x_i} - \frac{2}{3}\delta_{ij}\frac{\partial u_k}{\partial x_k}\right)\right] + \frac{\partial}{\partial x_j}\left(-\overline{\rho u_i' u_j'}\right), \tag{3}$$

$$\frac{\partial}{\partial x_i}\left[u_i\rho\left(h + \frac{1}{2}u_j u_j\right)\right] = \frac{\partial}{\partial x_j}\left[k_{\text{eff}}\frac{\partial T}{\partial x_j} + u_i(\tau_{ij})_{\text{eff}}\right],$$

$$k_{\text{eff}} = K + \frac{c_p \mu_t}{\text{Pr}_t}. \tag{4}$$

Since we assumed the working fluid is an ideal gas, then the compressibility effect must be imposed so that:

$$p = \rho R T. \tag{5}$$

The turbulence kinetic energy (k) and the rate of dissipation (ε) are derived from the following equations:

$$\frac{\partial}{\partial t}(\rho k) + \frac{\partial}{\partial x_i}(\rho k u_i) = \frac{\partial}{\partial x_j}\left[\left(\mu + \frac{\mu_t}{\sigma_k}\right)\frac{\partial k}{\partial x_j}\right] + G_k + G_b - \rho\varepsilon - Y_M, \quad (6)$$

$$\frac{\partial}{\partial t}(\rho \varepsilon) + \frac{\partial}{\partial x_i}(\rho \varepsilon u_i) = \frac{\partial}{\partial x_j}\left[\left(\mu + \frac{\mu_t}{\sigma_\varepsilon}\right)\frac{\partial \varepsilon}{\partial x_j}\right] + C_{1\varepsilon}\frac{\varepsilon}{k}(G_k + C_{3_\varepsilon} G_b) - C_{2\varepsilon}\rho\frac{\varepsilon^2}{k}. \quad (7)$$

In these equations, G_k, G_b and Y_M represent the generation of turbulence kinetic energy due to the mean velocity gradients, the generation of turbulence kinetic energy due to buoyancy, and the contribution of the fluctuating dilatation in compressible turbulence to the overall dissipation rate, respectively. $C_{1\varepsilon}$ and $C_{2\varepsilon}$ are constants; σ_k and σ_ε are also the turbulent Prandtl numbers for k and ε. The turbulent (or eddy) viscosity, μ_t, is computed as follows:

$$\mu_t = \rho C_\mu \frac{k^2}{\varepsilon}, \quad (8)$$

where C_μ is a constant. The model constants $C_{1\varepsilon}$, $C_{2\varepsilon}$, C_μ, σ_k and σ_ε have the following default values:

$$C_{1\varepsilon} = 1.44, \quad C_{2\varepsilon} = 1.92, \quad C_\mu = 0.09,$$

$$\sigma_k = 1.0, \quad \sigma_\varepsilon = 1.3.$$

3. Physical model description

3.1. 3D CFD model

The created 3D CFD model is based on what was used by Skye et al. [9]. It is noteworthy that an Exair™ 708 slpm [16] vortex tube was used by Skye et al. [9] to take all the experimental data. Figure 2 depicts the schematically drawing of vortex tube used by Skye et al. [9]. The dimensional geometry of vortex tube has been summarized in Table 1.

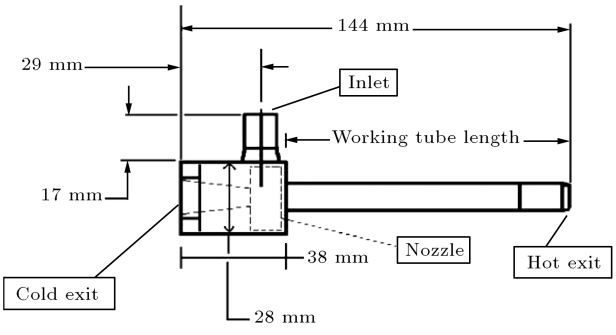

Figure 2. Schematic of vortex tube used by Skye et al. [9].

Table 1. Geometric summery of CFD models used for vortex tube.

Value	Measurement
Working tube length	106 mm
Vortex tube diameter	11.4 mm
Nozzle height	0.97 mm
Nozzle width	1.41 mm
Nozzle total inlet area (A_n)	8.2 mm^2
Cold exit diameter	6.2 mm
Cold exit area	30.3 mm^2
Hot exit diameter	11 mm
Hot exit area	95 mm^2

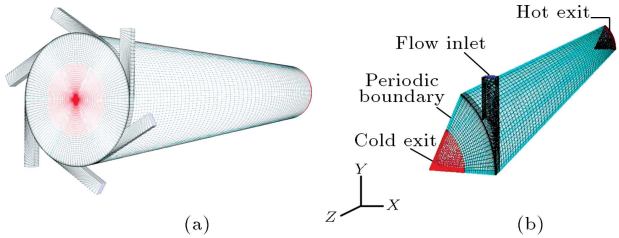

Figure 3. a) 3D CFD model of vortex tube with six straight nozzles. b) A sector of computational domain.

The 3D CFD mesh grid is shown in Figure 3(a). In this model, a regular organized mesh grid has been used. All radial line of this model of meshing has been connected to the centerline, and the circuit lines have been designed to be arranged from wall to centerline. So, the volume units that have been created in this model are regular cubic volumes. This meshing system helps the computations to be operated faster than the irregular and unorganized meshing, and the procedure of computations has been done more precisely.

Due to this reason that the computational domain is axisymmetric, the CFD model has been assumed to be a rotational periodic condition. Hence, only a sector of the flow domain with angle of 60° needs to be considered for computations, as shown in Figure 3(b).

3.2. Boundary conditions

Boundary conditions for this study have been indicated in Figure 4. The inlet is modeled as mass-flow-inlet.

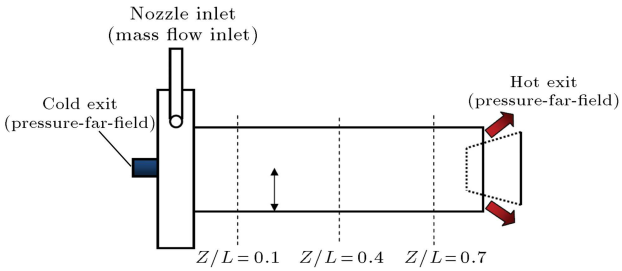

Figure 4. A schematic form of boundary conditions.

The inlet stagnation temperature and the total mass flow inlet are fixed to be 294.2 K and 8.35 g s^{-1}, respectively, according to the experimental conditions. A no-slip boundary condition is used on all walls of the system. For the cold and hot exits, two kinds of boundary conditions can be used for numerical analysis. The first boundary condition is pressure-outlet and the second one can be considered as pressure-far-field. The pressure-outlet boundary condition is used when the outlet pressures on both cold and hot outlets are known. However, the pressure-far-field boundary condition is used for the models with unknown outlet pressures.

In this article, both kinds of boundary conditions are used for cold and hot exits. For pressure-outlet boundary condition, the static pressure at the cold exit boundary was fixed at experimental measurement pressures, and the static pressure at the hot exit boundary is adjusted in the way to vary the cold mass fraction. The pressure-far-field boundary condition which is also employed for both exhausts including hot and cold exit is a state when the static pressures at the exhausts of vortex tube are not determined exactly. On the other hand, a vortex tube works in the ambient condition, and for change in the cold mass fraction, one needs to change the area of hot exit that is the true action for this purpose in comparison with pressure-outlet boundary condition. In this article, both kinds of boundary conditions are applied and investigated numerically, and the results are compared with each other.

A compressible form of the Navier-Stokes equation along with the standard k-ε model by second order upwind for momentum, turbulence and energy equations has been used to simulate the phenomenon of flow pattern and temperature separation in a vortex tube with 6 straight inlet nozzles operating under the condition of using different inlet gases by using the FLUENT^{TM} software package.

4. Results

4.1. The effect of different boundary conditions

The previous CFD researches on vortex tube have usually been performed in the fixed boundary condition such as pressure at the hot and cold exits. These values of pressure at exhausts are taken from experimental process that has been achieved during the experiment procedure. Since these pressures are not always available, this paper utilizes a useful method with any necessity of pressure values at cold and hot exits. This method is useful and suitable for CFD researchers which are involved in vortex tube fields. In this method, the pressure values of exhausts in the vortex tube are not necessary to be available, and the prediction is independent of pressure values at the exhausts. In the method presented in this paper, the pressure boundary condition is adjusted as pressure-far-field condition. This means that the vortex tube is working in ambient conditions. In order to achieve the certain cold mass fraction, we have to change the area of hot exhaust. In the real state (experimental), changing the hot exit area is achieved by the action of hot control valve.

In this section, for exhaust, both kinds of boundary conditions, i.e. pressure-far-field boundary and pressure-outlet boundary conditions are applied to the CFD model together with other boundary conditions for inlet, wall and periodic planes described in Section 3.2; cold and hot exit temperatures are derived and compared with experimental data to demonstrate that there is not noticeable difference between these two kinds of boundary conditions. As seen in Figures 5 and 6, cold and hot exit temperatures for both boundary conditions as a function of cold mass fraction (α) have good agreement with the experimental data. The presented data in Figures 5 and 6 are the minimum and maximum temperature achieved for cold and hot exits, respectively. In Figure 5, the minimum T_c is obtained at α about 0.3, through the experiment and CFD simulations. The applied 3D CFD model can produce hot gas temperature of 365.34 K at $\alpha = 0.82$ and a minimum cold gas temperature of 250.24 K at α about 0.3 cold mass fraction. It should be mentioned that the validation part has been done for compressed air.

In order to complete the comparison between pressure-outlet and pressure-far-field boundary conditions, some parameters such as axial velocity, tangential velocity, total pressure and total temperature at three different axial sections ($z/L = 0.1$, 0.4 and 0.7 have been defined in Figure 4) of the working tube

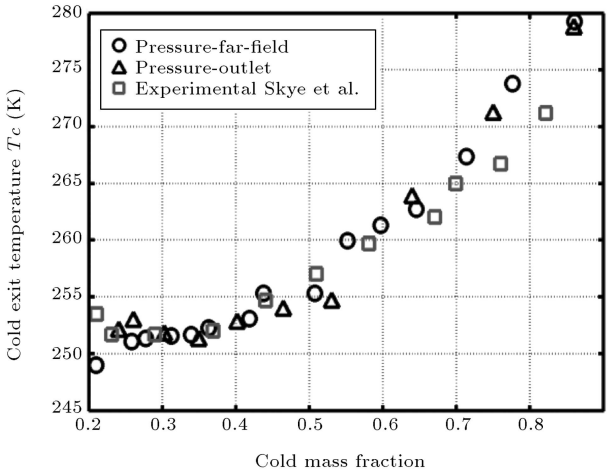

Figure 5. Comparison of cold exit temperature for both kinds of exhausts boundary conditions with the experimental data.

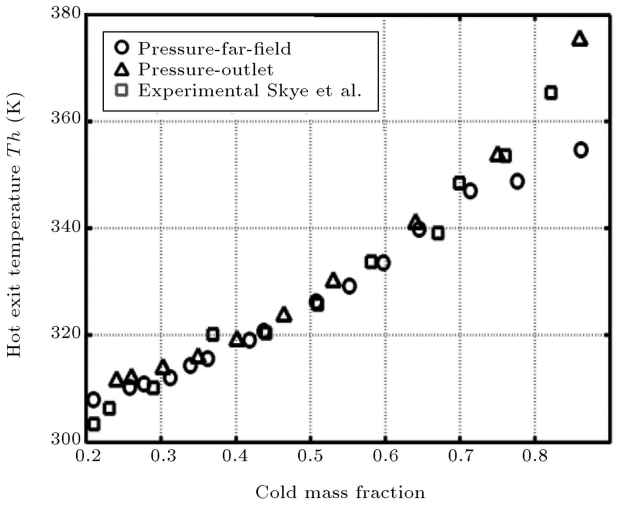

Figure 6. Comparison of hot exit temperature for both kinds of exhaust boundary conditions with the experimental data.

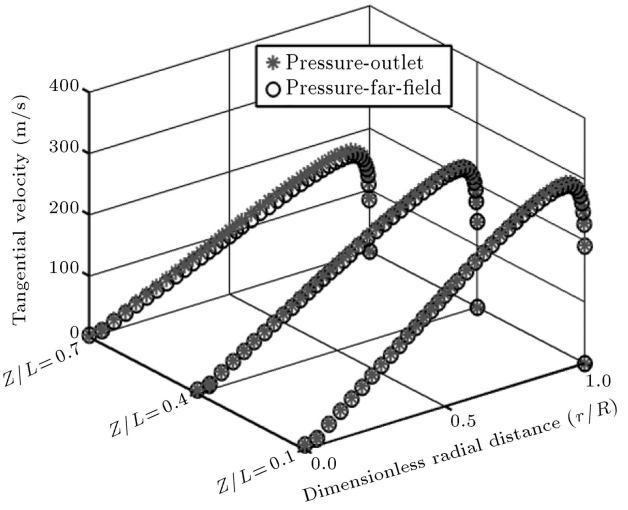

Figure 8. Indication of tangential velocity at different axial locations for two different boundary conditions .

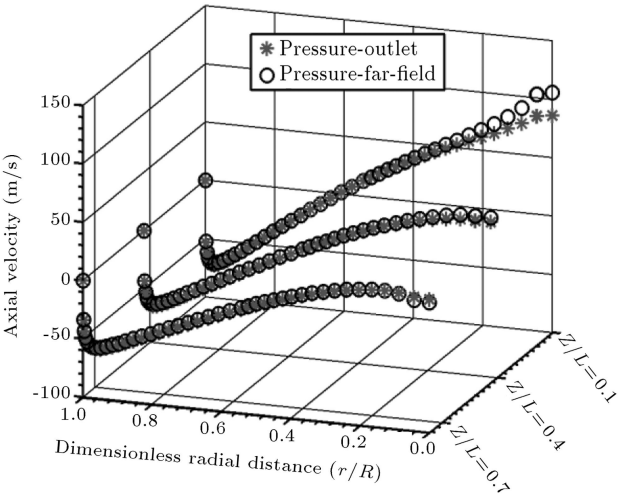

Figure 7. Indication of axial velocity at different axial locations for two different boundary conditions.

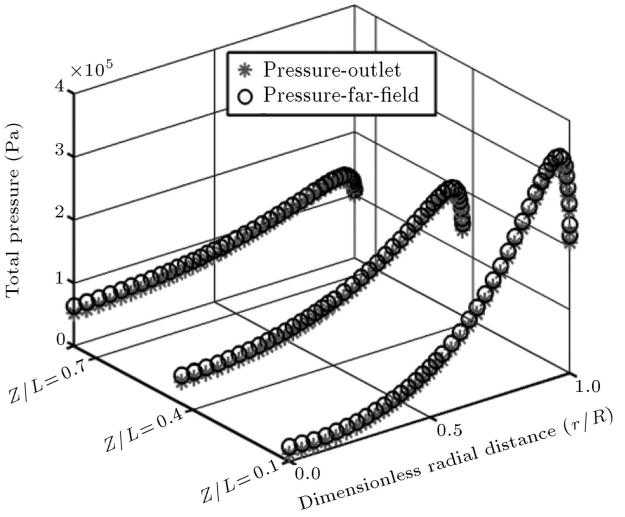

Figure 9. Indication of total pressure at different axial locations for two different boundary conditions.

have been studied as a function of dimensionless radial distance (r/R); meanwhile, the total temperature on the wall of vortex tube has been investigated.

The axial and tangential velocity, total pressure and total temperature distribution in different axial sections have been shown in Figures 7-10. In these figures, CFD results are compared by employing two different boundary conditions, and one can see good adjustability of the results for both models.

Figure 11 indicates the variation of total temperature on the tube wall for both pressure-far-field boundary and pressure-outlet boundary conditions in a comparative manner. In this case, also good agreement can be found for both CFD models.

Figures 7-11 prove that both mentioned kinds of boundary conditions have almost the same results and either of them can be used during the numerical process. As the pressure-far-field boundary condition does not need the outlet pressure, it is more usable in more situations in which the outlet pressures are not available. So, further in this research, the pressure-far-fielf boundary condition is used for all numerical computations.

4.2. Gridindependence study

The 3D CFD analysis has been performed for different average unit cell volumes in vortex tube as a computational domain. This is because the removing probable errors arise due to grid coarseness. Therefore, first the grid independence study has been done for $\alpha = 0.3$. As seen in the Figure 5, at this cold mass fraction, the vortex tube (with 6 straight nozzles) achieves a minimum outlet cold gas temperature. Consequently, in most of the evaluations, we use $\alpha = 0.3$ as a special value of cold mass fraction.

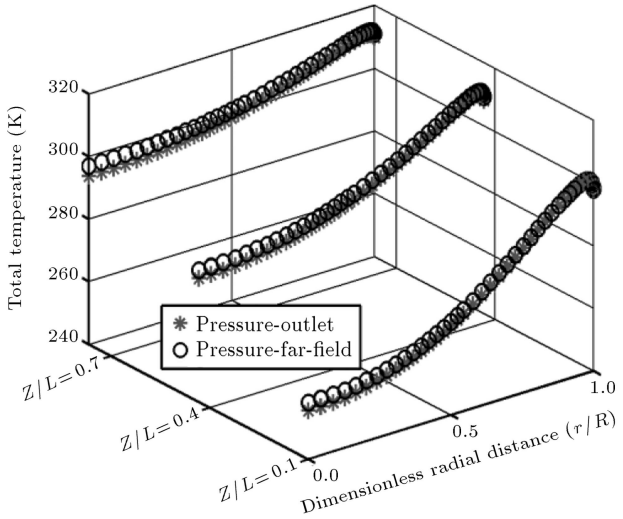

Figure 10. Indication of total temperature at different axial locations for two different boundary conditions.

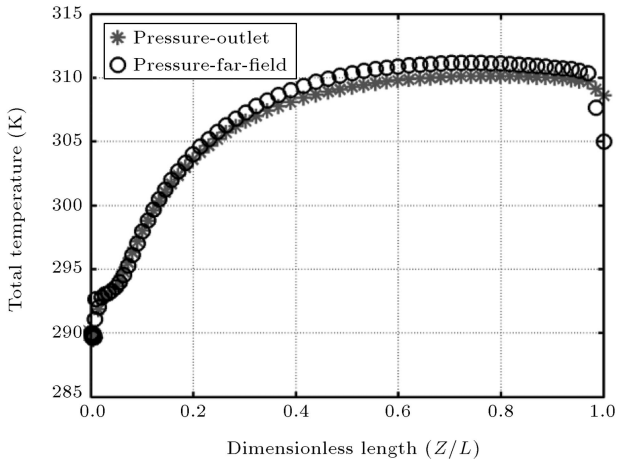

Figure 11. Indication of total temperature at tube wall for two different boundary conditions.

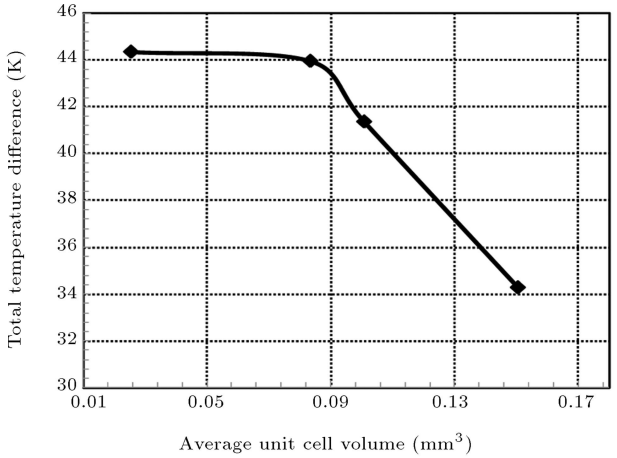

Figure 12. Grid size independence study on total temperature difference at different average unit cell volume.

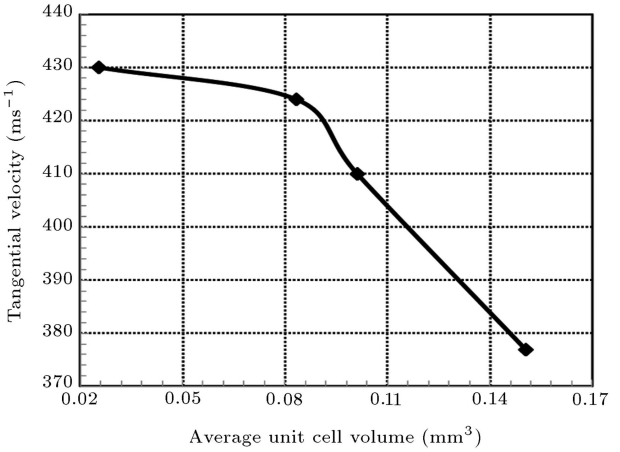

Figure 13. Grid size independence study on maximum swirl velocity at different average unit cell volume.

The variation of cold exit temperature difference and maximum tangential velocity as the main parameters are shown in Figures 12 and 13 respectively for different unit cell volumes. Not much major advantage can be seen in reducing of the unit cell volume size below 0.0257 mm^3, which corresponds to 287000 cells. The same type of unit cell volume of grids is used to study the introduced vortex tube with different type of gases.

4.3. The effect of different inlet gases

In the present study, the thermal performance of a vortex tube in the terms of cold and hot exit temperatures (T_c and T_h) and cold and hot power separation rates ($\dot{Q}_c$ and $\dot{Q}_h$) is predicted numerically. This prediction is based on different gases that have been employed in the operation of the vortex tube system.

The obtained total temperature distribution contours are portrayed in Figure 14, which represent the peripheral flow to be warmer and core flow to be cooler, in respect to the inlet temperature (294.2 K). Under operating condition of 8.34 g s^{-1}, maximum hot gas temperature of 311.5 K and minimum cold gas temperature of 250.24 K are produced for a vortex tube working with compressed air. The total temperature contour plotted in Figure 14 is related to $\alpha = 0.3$, which is obtained by the maximum cooling capacity of machine for air.

The main objective of this investigation is to achieve maximum cooling and heating capacity by changing the type of gas in the commercial vortex tube. Figure 15 shows the variation of temperature at the cold exit as a function of cold mass fraction. As seen in Figure 15, the behavior of experimental curve shows that the cold exit temperature increases with an increase in the cold mass fraction for amounts greater than 0.36. The obtained results for 3D CFD model show a good agreement behavior with experimental curve, which has taken air as working fluid in the

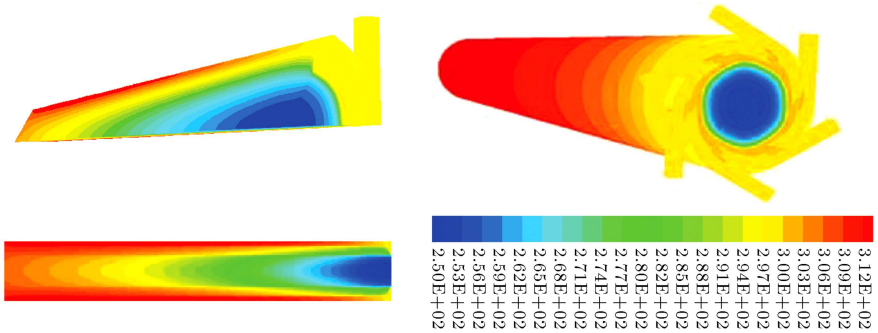

Figure 14. Temperature distribution in vortex tube working with compressed air, $\alpha = 0.3$.

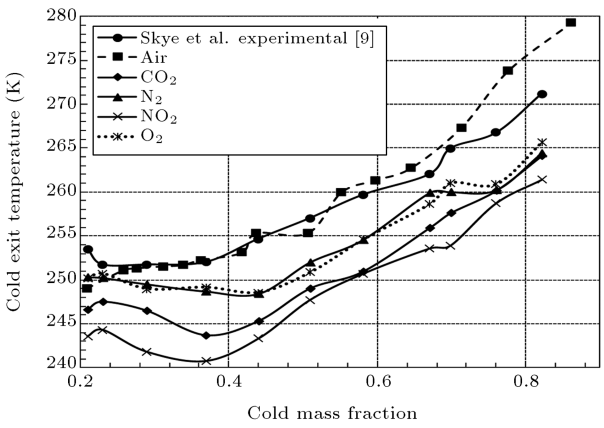

Figure 15. Variation of the cold exit temperature as a function of cold mass fraction for different types of inlet gases.

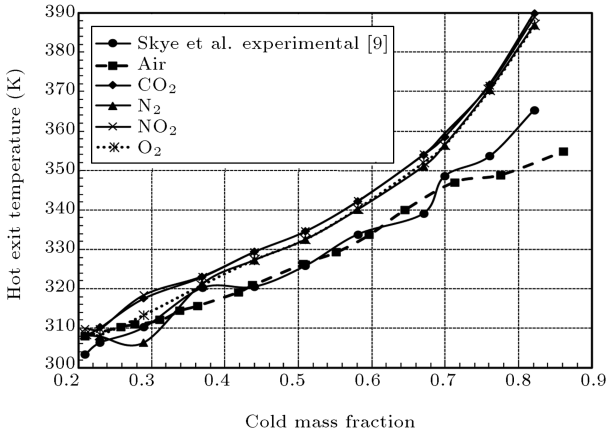

Figure 16. Variation of the hot exit temperature as a function of cold mass fraction for different types of inlet gases.

system. The other types of gases including NO_2, CO_2, N_2 and O_2 indicate lower temperature at the cold exit of vortex tube, which is desired. Among all the investigated gases, NO_2 shows the minimum amount of cold temperature, especially for $\alpha = 0.37$ which is equal to 240.73 K.

This prediction emphasizes that when the vortex tube is utilized as a refrigerator device, nitrogen dioxide (NO_2) is the best choice between the mentioned gases because of producing a lower temperature in comparison with the other gases. The minimum value of cold exit temperature for all gases is found to be located in cold mass fraction range of 0.29-0.37. Figure 16 illustrates the behavior of temperature curves of hot gas that exit from hot exhaust as a function of cold mass fraction.

As shown in Figure 16, different gases have the same treatment at the hot exit temperature distribution for different cold mass fractions. The hot exit temperature increases with an increase in the cold mass fraction in all models. Figure 16 indicates that there is no difference between the mentioned gases (rather than air), if the vortex tube has been used to obtain the warm gas from hot exit. Therefore, a gas with lowest cost can be chosed as there is no difference between gases in heating point of view. The temperature range of hot gas that exits from hot exhaust is found between 309.89 K and 388.86 K. Table 2 summarized the numerical results of cold and hot exit temperature (T_c and T_h) and their differences (ΔT_c and ΔT_h) for all types of inlet gases at a sample cold mass fraction, $\alpha = 0.3$. The results show the maximum amounts of $\Delta T_c = 39.8$ K and $\Delta T_h = 14.14$ for NO_2 among the investigated cases.

According to the obtained results from temperature separation reports, a suggestion for using the investigated gases is represented in Table 3 for cooling or heating purposes. The gases producing higher amount of ΔT_c and ΔT_h are placed in the upper cells of Table 3. Although from economical point of view it seems that air is more appropriate to be used in a vortex tube system because of having free cost, investigations show the higher capability of other gases in producing cooling or heating streams in respect to compressed air.

Another parameter that illustrates the performance of a vortex tube is the energy separation rate at cold and hot exits ($\dot{Q}_c$ and $\dot{Q}_h$), which is one of the main concepts in vortex tube. $\dot{Q}_c$ and $\dot{Q}_h$ can be evaluated as follows:

Table 2. Total temperature separation at cold mass fraction, $\alpha = 0.3$, in the CFD models.

Type of gas	Cold exit temperature (K)	Hot exit temperature (K)	ΔT_c (K)	ΔT_h (K)	ΔT_t (K)
Air	250.24	311.5	43.96	17.3	61.26
CO_2	246.48	317.5	47.72	23.3	71.02
N_2	249.48	306.42	44.72	12.22	56.94
NO_2	241.08	318.33	53.12	24.13	77.25
O_2	248.95	313.28	45.25	19.08	64.33

Table 3. Arrangement of gases in the capability of temperature separation enhancement.

Superiority of type of gas for cooling	Superiority of type of gas for heating
NO_2	NO_2
CO_2	CO_2
O_2	O_2
N_2	Air
Air	N_2

$$\dot{Q}_c = \dot{m}_c c_p (T_i - T_c), \tag{9}$$

$$\dot{Q}_h = \dot{m}_h c_p (T_h - T_i), \tag{10}$$

where c_p is the specific heat of the gas.

$\dot{Q}_c$ and $\dot{Q}_h$ in the vortex tube have been shown in Figures 17 and 18. Both the experimental data and CFD models show maximum power separation with a cold fraction of about 0.65. The rate of energy separation is observed to increase with an increase in cold mass fraction in the range of 0.21-0.65. Over this range of cold mass fraction, the energy separation is observed to decrease with an increase in the cold mass fraction.

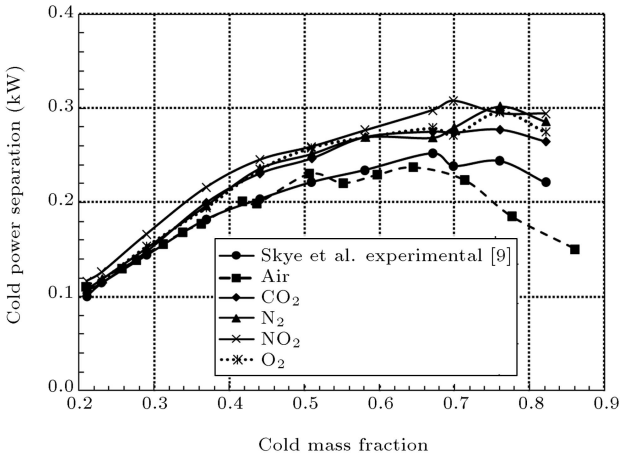

Figure 17. Comparison of cold energy separation rate with experimental data for different gas types.

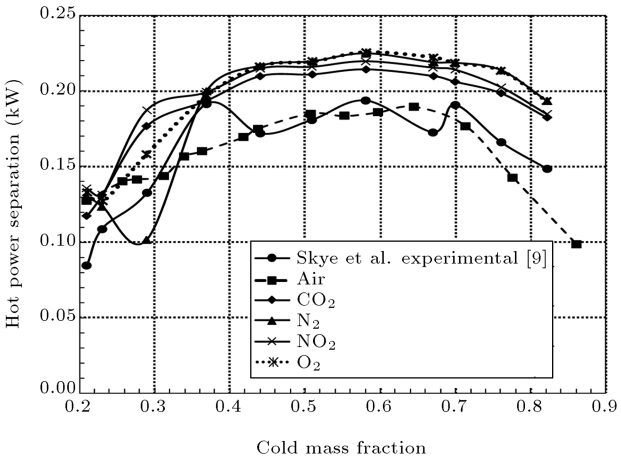

Figure 18. Comparison of hot energy separation rate with experimental data for different gas types.

5. Conclusion

In the present research, a 3D CFD model was used for applying as a predictive tool in the investigation of a vortex tube performance. The 3D computational fluid dynamic model used in this study is a steady axisymmetric model that employs standard k-ε turbulence model to perform the computation procedure of results. Using different gases in the vortex tube for cooling and heating applications was the main subject of this article. Results of this study help researchers to use the vortex tube in cooling or heating industries to choose the best type of gas to achieve the appropriate condition. As a conclusion, for cooling or refrigerating a special zone by means of a vortex tube, nitrogen dioxide (NO_2) gas produces the maximum amount of cooling performance, because it creates a colder stream in comparison with other gases. A comprehensive comparison was performed in this article between two different kinds of boundary conditions for cold and hot exhausts, i.e. pressure-outlet and pressure-far-field. The results confirmed that almost there is no difference between the obtained numerical results from those types of boundary conditions. In addition, both mentioned boundary conditions follow the experimental results as well. When the vortex tube is used as a heating device, the best choice for fluid system, to achieve the highest efficiency and temperature, is

NO_2 again. Comparison of the present numerical results with the measured experimental data, revealed a reasonable agreement.

Nomenclature

D	Diameter of vortex tube (mm)
K	Turbulence kinetic energy (m^2s^{-2})
L	Length of vortex tube (mm)
r	Radial distance from the centerline (mm)
T	Temperature (K)
T_i	Inlet gas temperature (K)
Z	Axial length from nozzle cross section (mm)
$\dot{m}$	Mass flow rate (kg s^{-1})

Subscripts

i	Inlet
c	Cold
h	Hot
t	Total

Greek Symbols

α	Cold mass fraction
ε	Turbulence dissipation rate (m^2 s^{-3})
ΔT	Temperature difference (K)
ρ	Density (kg m^{-3})
σ	Stress (N m^{-2})
μ	Dynamic viscosity (kg m^{-1} s^{-1})
μ_t	Turbulent viscosity (kg m^{-1} s^{-1})
τ	Shear stress (N m^{-2})
τ_{ij}	Stress tensor components

References

1. Ranque, G.J. "Experiments on expansion in a vortex with simultaneous exhaust of hot air and cold air", *Le J. de Phys., et le Radium.*, **4**, pp. 112-114 (in France) (1933).
2. Hilsch, R. "The use of expansion of gases in a centrifugal field as a cooling process", *Rev. Sci. Instrum.*, **18**, pp. 108-113 (1947) (in German).
3. Kurosaka, M. "Acoustic streaming in swirling flows", *J. Fluid Mech.*, **124**, pp. 139-172 (1982).
4. Stephan, K., Lin, S., Durst, M., Huang, F. and Seher, D. "An investigation of energy separation in a vortex tube", *Int. J. Heat Mass Trans.*, **26**, pp. 341-348 (1983).
5. Dincer, K., Baskaya, S. and Uysal, B.Z. "Experimental investigation of the effects of length to diameter ratio and nozzle number on the performance of counter flow Ranque-Hilsch vortex tubes", *Heat Mass Trans.*, **44**, pp. 367-373 (2008).
6. Ahlborn, B.K. and Gordon, J.M. "The vortex tube as a classic thermodynamic refrigeration cycle", *J. Appl. Phys.*, **88**, pp. 3645-3653 (2000).
7. Akhesmeh, S., Pourmahmoud, N. and Sedgi, H. "Numerical study of the temperature separation in the Ranque-Hilsch vortex tube", *Am. J. Eng. Appl. Sci.*, **3**, pp. 181-187 (2008).
8. Aljuwayhel, N.F., Nellis, G.F. and Klein, S.A. "Parametric and internal study of the vortex tube using a CFD model", *Int. J. Refrig.*, **28**, pp. 442-450 (2005).
9. Skye, H.M., Nellis, G.F. and Klein, S.A. "Comparison of CFD analysis to empirical data in a commercial vortex tube", *Int. J. Refrig.*, **29**, pp. 71-80 (2006).
10. Bramo, A.R. and Pourmahmoud, N. "Computational fluid dynamics simulation of length to diameter ratio effect on the energy separation in a vortex tube", *Therm. Sci.*, **15**, pp. 833-848 (2011).
11. Chang, H.S. "Experimental and numerical studies in a vortex tube", *J. Mech. Sci. Tech.*, **20**, pp. 418-425 (2006).
12. Polat, K. and Kirmaci, V. "Determining of gas type in counter flow vortex tube using pairwise fisher score attribute reduction method", *Int. J. Refrig.*, **34**, pp. 1372-1386 (2011).
13. Pourmahmoud, N., Hassan Zadeh, A., Moutaby, O. and Bramo, A.R. "CFD analysis of helical nozzles effects on the energy separation in a vortex tube", *Therm. Sci.*, **16**, pp. 149-164 (2012).
14. Pourmahmoud, N., Hassan Zadeh, A. and Moutaby,O. "Numerical analysis of the effect of helical nozzles gap on the cooling capacity of Ranque-Hilsch vortex tube", *Int. J. Refrig.*, **35**, pp. 1473-1483 (2012).
15. Khazaei, N., Teymourtash, A.R. and Jafarian, M.M. "Effects of gas properties and geometrical parameters on performance of a vortex tube", *Scientia Iranica, Transactions B: Mechanical Engineering*, 19, pp. 454-462 (2012).
16. Exair Corporation. *Vortex Tubes and Spot Cooling Products*. Available at [http://www.exair.com]

Biographies

Nader Pourmahmoud was born in 1969 in Iran. He received his BS degree in Mechanical Engineering from Shiraz University in 1992. After achieving some practical engineering projects till 1997, he started his MSc degree in Mechanical Engineering (energy conversion field) in Tarbiat Modarres University in Tehran, and finally he received his PhD degree in

Mechanical Engineering (energy conversion field) in 2003 at the same university. He has joined the Faculty of Engineering of Urmia University since 2003, where he is an Associate Professor in the Mechanical Engineering Department. His professional interest is in the field of CFD of Turbulent fluid flow, energy conversion problems and especially in the vortex tube.

Seyed Ehsan Rafiee has been an MSc student at the Institute of Energy Conversion (Mechanical Engineering), Urmia University of Technology, Urmia, Iran, since 2011. His research interests are in in the area of numerical analysis for the solution of Fluid Flow PDEs and Computational Fluid Dynamics (CFD).

Masoud Rahimi has been an MSc student at the Institute of Energy Conversion (Mechanical Engineering), Urmia University of Technology, Urmia, Iran, since 2011. His research interests are in the area of numerical analysis.

Amir Hassanzadeh was born in 1986, in Iran. He received his BS degree in Mechanical Engineering in Kashan University in 2009. In the same year, he started his MSc degree in Mechanical Engineering (energy conversion field) in Urmia University. He has been a PhD student in Urmia University, since 2012. His research interests are in the area of numerical analysis of fluid mechanics problems.